

5-1-2012

## Effects of Long-Range Tip-Sample Interaction on Magnetic Force Imaging: A Comparative Study Between Bimorph Driven System and Electrostatic Force Modulation

Byung I. Kim  
*Boise State University*

# Effects of Long-Range Tip-Sample Interaction on Magnetic Force Imaging: A Comparative Study Between Bimorph Driven System and Electrostatic Force Modulation

Byung I. Kim  
Boise State University

## Abstract

Magnetic force microscopy (MFM) using electrostatic force modulation has been designed and developed to avoid the drawbacks of the bimorph driven system. The bimorph driven system has poor frequency response and overlap of the topographic features on magnetic structures of the MFM images. In the electrostatic force modulation system, the amplitude increases in the noncontact regime as the tip approaches due to the capacitive coupling between tip and sample. MFM using electrostatic force modulation has been applied to observe maze-like stripe domain structures on a CoCr film. The contrast mechanism and imaging stability of MFM using electrostatic force modulation are discussed by investigating the force distance curves obtained in two magnetic domain regions.

**Keywords:** MFM, scanning probe microscope, electrostatic modulation, imaging stability, magnetic domain, long range interaction

## Introduction

Magnetic force microscopy (MFM) has matured and developed into a routine method for imaging magnetic surface structures<sup>1</sup>. Since magnetic forces between the tip and sample are very weak ( $\sim 10^{-12}$  N), an ac-mode operation with a small vibration amplitude between the tip and sample is used to detect these weak magnetic interactions<sup>2</sup>. When the oscillation amplitude is used as a feedback signal, the image obtained represents a constant force gradient contour of the magnetic sample surface. Most of the systems currently implemented in MFM are based on mechanically driven vibrations utilizing a piezo device called a bimorph (see **Fig. 1(a)**).

The bimorph-driven system is limited in its ability to separate the MFM signal from the topographic signal on surfaces where topographic features match or exceed the tip-height where imaging occurs<sup>3-5</sup>. Mixing of the topographic and magnetic signals can make it difficult to extract the intrinsic magnetic structure from MFM images, thereby limiting our understanding of magnetic surfaces. To circumvent this imaging limitation, an MFM method has recently been designed and developed using electrostatic force modulation to separate the magnetic domain structure from the topographic structure on magnetic samples with rough surfaces<sup>6</sup>. In this method, a capacitive coupling (an electrostatic attraction or repulsion via the capacitance between tip and sample) is introduced between the tip and sample using electrostatic force modulation (see **Fig. 1(b)**).

This paper describes the detailed mechanism of the stability improvement electrostatic force modulation (EFM) provides through a direct comparison of the amplitude-frequency curves produced by the bimorph and EFM methods when scanning a magnetic sample surface. The effects on imaging stability of tip-sample separation and perturbations (e.g., collisions between the cantilever tip and a tall hillock structure) were also investigated. The superior performance of the electrostatic force modulation system results from the long-range electrostatic capacitance effect and the direct force modulation effect.

## Materials and Methods

A CoCr magnetic film sample was deposited on a glass substrate by the dc magnetron sputtering method, up to thickness 300 nm. A heavily doped Si cantilever coated with a magnetic Co thin layer was used (Nanosensors). The cantilever has a force constant of 2.1 N/m and its resonant frequency is about 106 kHz. The tip was magnetized by placing the cantilever in a magnetic field of 0.2 T, aligned perpendicularly to the lever, for 3 minutes. The electrical contact for the tip and sample was made with a silver paste. The average height of the tip during bimorph driven modulation with an amplitude of 85 nm

was 150 nm, while during electrostatic force modulation with an amplitude of 95 nm the average height of the tip was 170 nm.

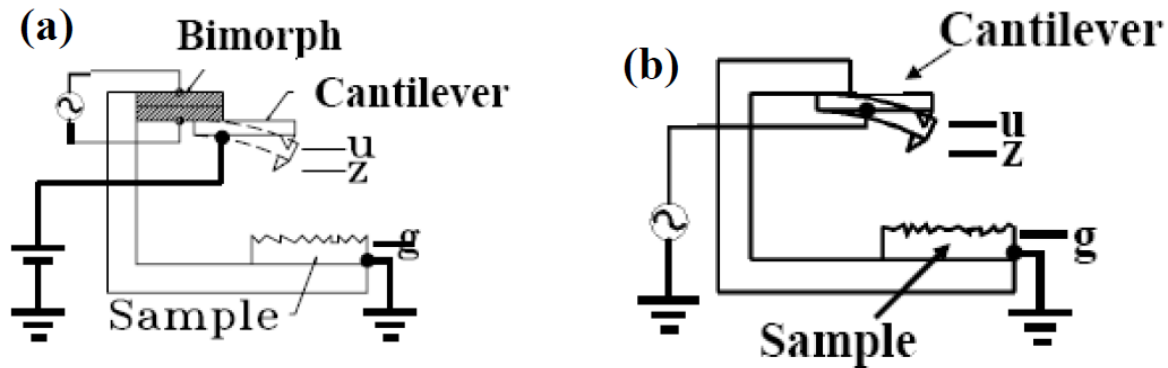


**Figure 1.** (a) Schematic of the bimorph driven system. (b) Schematic of the electrostatic force modulation system.

For MFM imaging using the bimorph driven method in **Fig. 1(a)**, a dc voltage +10V was applied between tip and sample to provide the servo force  $F_C$  for feedback to keep the tip from crashing into the surface during scanning<sup>7</sup>. For the electrostatic force modulation method in **Fig. 1(b)**, a sinusoidal signal  $V_{ac}\sin(\omega t)$  was applied using a function generator (Hewlett Packard, HP 33120A) to modulate the gap between the tip and sample. The  $\omega$  represents the angular frequency or the rate of the phase change of the inputted sinusoidal modulation. In this experiment, we applied a  $V_{ac}$  of 14 V between the tip and sample surface at an operating frequency 53 kHz, half the resonance frequency of the cantilever. For both magnetic imaging methods, magnetic and topographic images were obtained under a constant amplitude feedback condition by using the difference between the output of the amplitude and set-amplitude as the error signal. The typical scan rate was 1 Hz. All data was obtained using commercial atomic force microscopy (AFM) (Park Scientific AutoProbe LS) in air.

## Results

**Figures 2(a)** and **2(b)** compare the amplitude-frequency curves for the two MFM systems. In the bimorph driven system (**Fig. 2(a)**), unwanted peaks around the cantilever resonance result in unstable feedback conditions during MFM imaging. This poor frequency response of the cantilever is due to the additional frequency components integrated near the primary resonance peak, as shown in **Fig. 2(a)**. The existence of several resonance peaks imposes drastic restrictions on the operating frequency range at which useful measurements can be made. In the electrostatic force modulation system (**Fig. 2(b)**), the cantilever frequency response has two well-defined resonance peaks. This indicates that the cantilever is the only component being driven by electrostatic force modulation.

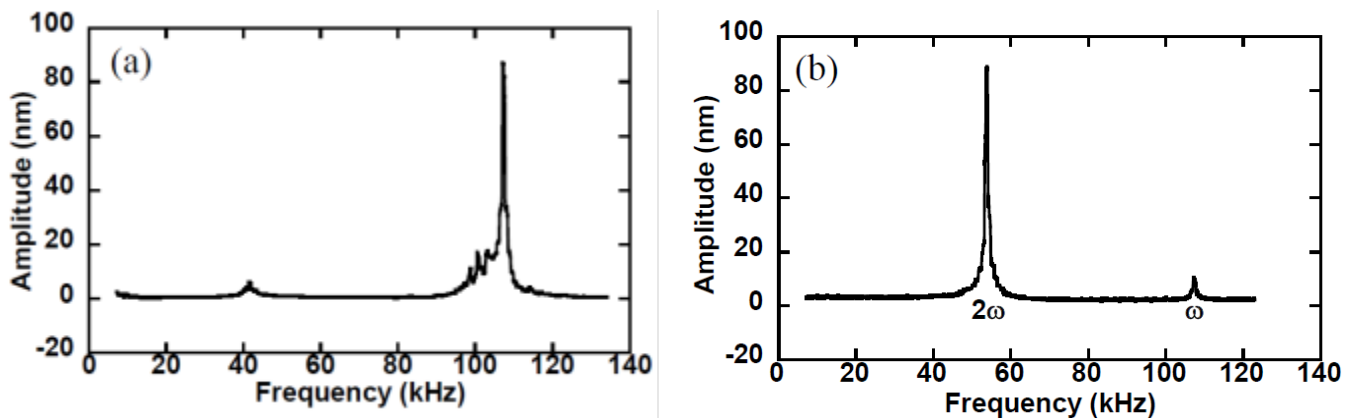


**Figure 2.** Amplitude vs. frequency response for the cantilever. (a) The bimorph driven system. (b) The electrostatic force modulation system.

**Figures 3(a)** and **3(b)** show maze-like magnetic domain structures with periodicity 3 to 5  $\mu\text{m}$  obtained by MFM using bimorph driven and electrostatic force modulations, respectively. The dotted lines represent areas where sectional profiles (presented in the Discussion section) of the magnetic features are taken. These results are consistent with our previous study<sup>6</sup>. However, topographic features frequently overlap in magnetic images, as shown in **Fig. 3(a)**. The overlapped topographic features appear to be associated with previously observed large hillocks with diameter 5 to 10  $\mu\text{m}$  and height 100-300 nm<sup>6</sup>. **Figure 3(b)** shows an MFM image of the striped magnetic domains on the CoCr magnetic film. We reproduced the same image repeatedly at the same location, indicating the improved stability of the electrostatic force modulation technique.

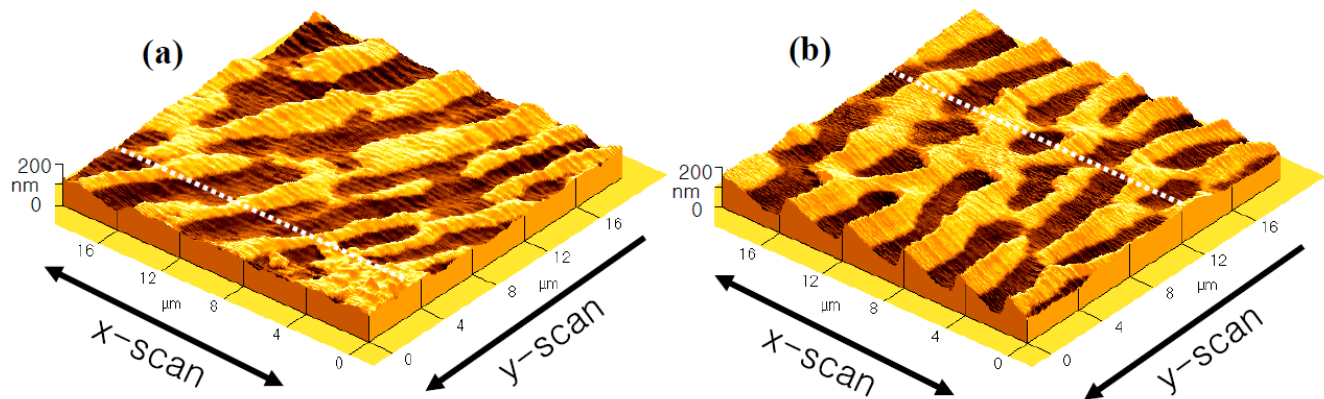


**Figure 3.** MFM images showing maze-like magnetic domain structures with periodicity 3 to 5  $\mu\text{m}$  (scan area: 20  $\mu\text{m}$  x 20  $\mu\text{m}$ ) taken with bimorph driven system **(a)** and electrostatic force modulation system **(b)**.

**Figures 4(a)** and **4(b)** illustrate the differences in imaging stability obtained by bimorph and electrostatic MFM systems. **Figure 4(a)** shows an MFM image of stripe domain structures with an average surface roughness of approximately 45 nm and periodicity 4.5–5  $\mu\text{m}$  on CoCr magnetic film, consistent with previously reported MFM images<sup>8</sup>. As the bimorph-driven tip scans over the magnetic surface, it appears to crash into a large hillock which is taller than the tip height. The crash of the tip and a hillock structure (as marked by an arrow in the middle of y-scan) creates a feedback disturbance, overcoming the barrier for the imaging mode transition from magnetic mode to topographic mode<sup>6</sup>. After the crash, the tip remains in tapping mode as it continues to scan in the y-direction<sup>9</sup>. The topographic image mode stays until the tip completes scanning, different from previous observations of reversible switches between noncontact and topographic mode<sup>6,10</sup>. The persistence of topographic imaging mode in the bimorph driven system indicates that there is a hysteresis in switching between tapping mode and the noncontact magnetic mode. This irreversible process indicates that there might be a change in the energy barrier between the noncontact and tapping regions in the amplitude-distance curve. The disappearance of noncontact mode in **Fig. 4(a)** can possibly be explained by a change in the tip structure during the crash.<sup>11</sup> **Figure 4(b)** shows a magnetic image from the same sample surface, this time using electrostatic force modulation. The image exhibits an average surface roughness of approximately 70 nm. As the electrostatically driven tip scans over the magnetic surface, it again encounters the large hillock which is taller than the tip height. After the encounter, the tip stays in noncontact mode as it scans in the y-direction. The persistence of noncontact mode in the electrostatically driven system can possibly be understood by the opposite polarity of slope of the amplitude-distance curve in the tapping and noncontact regions<sup>6</sup>. In addition, the completeness of the magnetic image beyond the encounter indicates that the enhanced barrier height in amplitude (i.e. the difference between peak height and the horizontal set-amplitude) of the electrostatic force modulation system (over the bimorph system) prevents the cantilever from snapping upon contact with the surface. Since there are no appreciable height changes in the magnetic image, the tip appears to be more secure under the electrostatically modulated system.

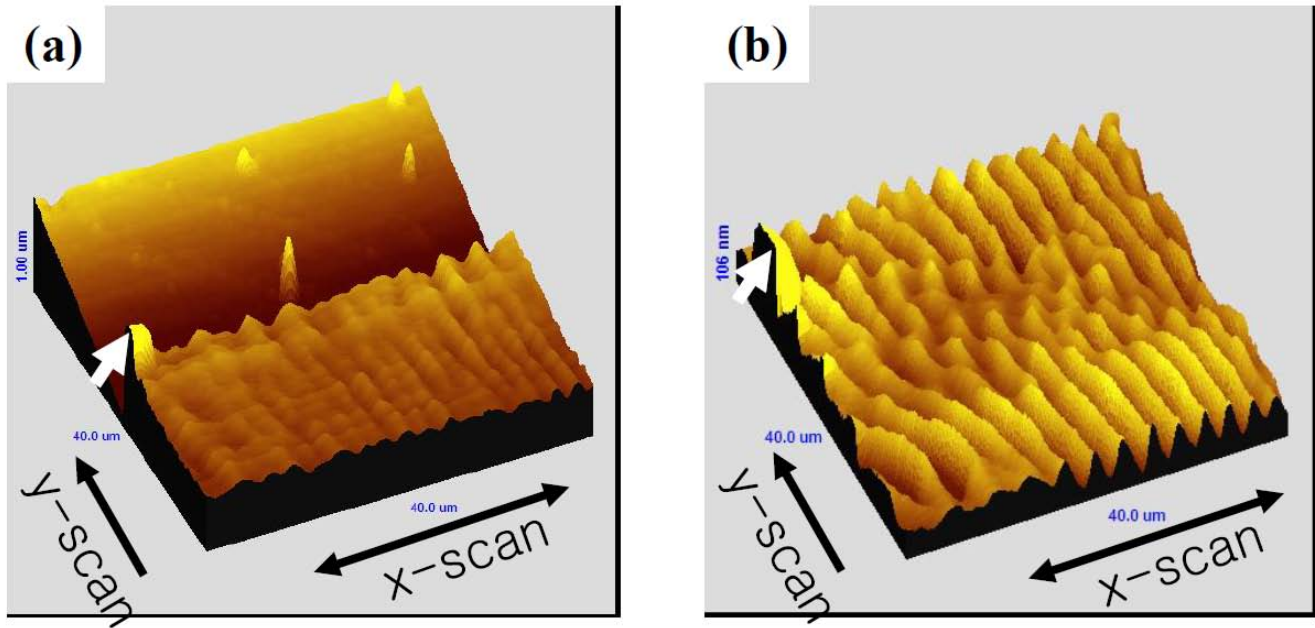


**Figure 4.** (a) Transition from magnetic domain imaging mode to topographic imaging mode during tip-scanning of CoCr film with set-amplitude 85 nm using bimorph driven modulation (scan area: 40  $\mu\text{m}$  x 40  $\mu\text{m}$ ). The bimorph driven system is more susceptible to large topographic features such as the feature indicated by an arrow, which causes the imaging mode to change from magnetic to topographic. (b) Magnetic domain image of CoCr film in the noncontact regime with set-amplitude 95 nm operating at the resonance frequency 53 kHz using the electrostatic force modulation system (scan area: 40  $\mu\text{m}$  x 40  $\mu\text{m}$ ). The system is robust against frequent tip-collisions with topographic hillocks such as the feature indicated by an arrow.

### Discussion

**Figure 5(a)** shows the amplitude change as the tip approaches the sample surface in the bimorph driven system. As the distance decreases, the amplitude decreases monotonously in the noncontact region and continues to decrease in an oscillatory pattern in the tapping region. It is important to note that the feedback polarity is the same in both the noncontact and tapping regimes in the bimorph driven system. For a given set-amplitude, two stable oscillatory cantilever motions are possible. This bistable states are graphically represented in **Fig. 5(a)** by the two interacting points between the curve data and the horizontal dotted line which represents set-amplitude under feedback<sup>6</sup>. The overlap of the topographic signal onto the magnetic signal during scanning resulted from the feedback bistability between the noncontact and tapping regions in the amplitude-distance curve. Therefore, the sudden disappearance of magnetic structures in **Fig. 4(a)** can be understood as a transition from the bistable states to a monostable tapping state due to the possible decrease of the tip radius. The decrease causes the noncontact region of the amplitude-distance curve to move upward due to a capacitance decrease.<sup>11</sup>

The amplitude-distance curve obtained with the electrostatic modulation system is very different from the one in the bimorph driven system. **Figure 5(b)** shows the amplitude change as the tip approaches the sample surface in the electrostatic force modulation system. The amplitude increases in the noncontact region but decreases in the tapping region as the distance decreases.

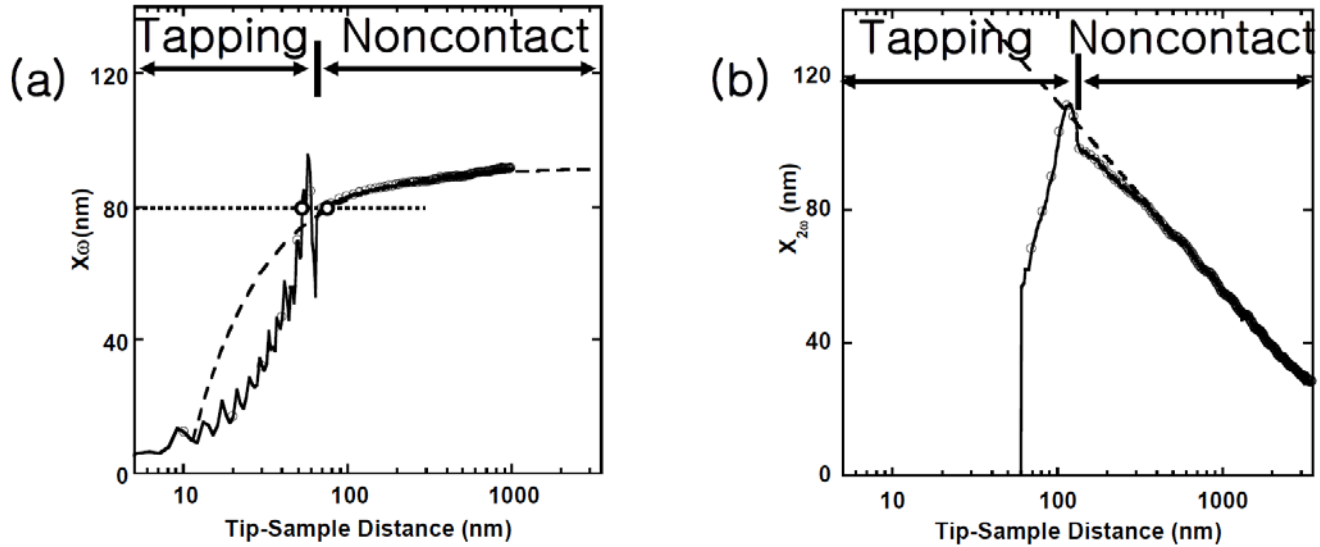


**Figure 5.** (a) Amplitude vs. distance data for the bimorph system. Note the identical feedback polarity in the noncontact and tapping regions. The dashed line fits the data with  $1/z$ . (b) Amplitude vs. distance data for the electrostatic force modulation system. Note the barrier between the noncontact and tapping regions and the opposite feedback polarity (sign of slope) in each region. The dashed line fits the data to the logarithmic function  $b \times \log(D/z)$ .

In the usual constant force gradient mode with bimorph driven modulation, a dc voltage is applied between the tip and sample to prevent the tip from crashing into the surface during scanning. Instead, we employ the electrostatic force modulation technique for self-actuation of the cantilever to satisfy the requirements for MFM imaging. This direct force modulation utilizes capacitive force coupling between the cantilever and the sample to induce the modulation (**Fig. 1(b)**). To avoid mixing of the topographic signal with the MFM image, we must increase the operating distance of the noncontact region to avoid the tip crashing near the tapping region. The opposite feedback polarity between noncontact mode and tapping mode is necessary to exclude possible mixing of topographic signal due to the tapping mode operation during noncontact MFM imaging. The electrostatic force keeps the total force gradient always positive for both repulsive and attractive magnetic forces. In **Fig 5(b)**, the decrease in amplitude results from the sudden involvement of the repulsive tapping force. The peak represents a transition from an electrostatic noncontact interaction to tapping interaction between the tip and the sample. The linear part in the tapping regime is used to find the amplitude of the tip vibration in the noncontact regime because the z-piezo is precisely calibrated<sup>8,12,13</sup>.

However, in the bimorph driven system, the linear tapping region also has the same sign of slope as the noncontact region<sup>6</sup>. This indicates that there exists two *stable* states for a given set-amplitude ( $X_{\omega,SP}$ ); one in the tapping region and the other in the noncontact region (as depicted in **Fig. 5(a)** by the dotted line at the amplitude of 80 nm, which intersects at the locations symbolized by the open circles). The coexistence of two stable states is analogous to that in the atomic force microscopy (AFM)<sup>8,12</sup>. Garcia and San Paulo associated continual switching of the oscillating tip between the two stable states with abrupt changes in height of topographic features.<sup>8</sup> Similarly, we attribute the appearance of topographic features in a magnetic image to the switching between the bi-stable states. When we performed the magnetic imaging as a function of feedback set-point amplitude  $X_{\omega,SP}$  at the same tip-location repeatedly, the pick-up ratio was found to depend upon the average distance of the noncontact state from the sample surface<sup>6</sup>. This result supports that this switching mechanism is the major channel of picking up topographic features in a magnetic image. Using electrostatic force modulation, tip-crashing toward the surface upon encountering the peak barrier in **Fig. 5(b)** rarely happens during repeated magnetic imaging. Hong et al. reported the same type of stable imaging condition in tapping mode AFM using the electrostatic force modulation<sup>14</sup>.

The equation of motion of the cantilever probe is employed to reveal the stability of the mechanism: the probe with a single-point mass undergoes one-dimensional forced harmonic oscillation along the vertical  $z$  axis in **Figs. 1(a)** and **1(b)** for bimorph driven modulation and electrostatic force modulation, respectively. This oscillation is described by the following equation:

$$\frac{\partial^2 z}{\partial t^2} + \frac{\omega_0}{Q} \frac{\partial z}{\partial t} + \omega_0^2 (z - u) = \frac{1}{m} (F_m + F_C + F_{vdw}) \quad (1)$$

where  $z$  is the coordinate perpendicular to the sample surface,  $t$  is time,  $u$  is the undeflected cantilever position,  $m$  is the point mass (cantilever),  $\omega_0$  is the resonance angular frequency,  $Q$  is the quality factor, and  $\omega_0/Q$  corresponds to the damping constant per unit mass in the presence of magnetic force  $F_m$ , capacitance force  $F_C$ , and Van der Waals force  $F_{vdw}$ . Equation (1) can be solved analytically when the average tip-sample distance  $u$  is much bigger than the set-amplitude  $X_{\omega,SP}$ , for both bimorph driven and electrostatic force modulation systems. The equation of motion (1) has  $u$  being constant while ac voltage is applied.

For electrostatic force modulation, the square law dependence of the capacitive force  $F_C$  on the driving signal  $V_{ac} \cos(\omega t)$  induces a mechanical vibration of the cantilever:

$$F_C = \frac{1}{4} \frac{\partial C}{\partial z} V_{ac}^2 (1 + \cos 2\omega t) \quad (2)$$

where  $C$  is the capacitance between tip and sample. The in-phase amplitude of the  $2\omega$  component,  $X_{2\omega}$ , is predicted as follows:

$$X_{2\omega} = \frac{1}{2m} \frac{-2F_C(z, V_{ac})(\omega_0'^2 - 4\omega^2)}{\sqrt{(\omega_0'^2 - 4\omega^2)^2 + \left(\frac{2\omega\omega_0}{Q}\right)^2}} \sin(\phi_{2\omega} + \phi_0) \quad (3)$$

where  $\phi_0$  is  $108^\circ$  which maximizes the  $X_{2\omega}$  near  $u = 100$  nm.

$$\tan \phi_{2\omega} = \frac{2\omega\omega_0}{Q(\omega_0'^2 - 4\omega^2)} \quad (4)$$

where  $\omega_0'^2 = \omega_0^2 \left( 1 - \frac{1}{k} \left( F_m' + \frac{1}{2} F_C'(z, V_{ac}) \right) \right)$ ,

$$F_C(z, V_{ac}) = \frac{1}{2} \frac{\partial C}{\partial z} V_{ac}^2 \quad \text{and} \quad (5)$$

$$F_C'(z, V_{ac}) = \frac{1}{2} \frac{\partial^2 C}{\partial z^2} V_{ac}^2 \quad (6)$$

The Lorentzian equation (3) accounts for the behavior of  $X_{2\omega}$  in **Fig. 2(b)**. The above predicted solution is compared with the experimental data to find the dependence of the interaction with distance in **Fig. 5(b)**. The amplitude increases in the noncontact region using electrostatic force modulation since the change of the electrostatic capacitance force  $-F_C(z, V_{ac})$  in Eq. (3) increases as the distance  $z$  becomes smaller. Experimental data in **Fig. 5(b)** shows that the electrostatic interaction extends up to 3,000 nm (equivalent to the limit of our  $z$ -piezo). The dashed line of the prediction of Eq. (3) matches well with the experimental data in the distance range 200-4000 nm (over the entire noncontact region). In the prediction, the electrostatic capacitance force  $-F_C(z, V_{ac})$  is described by assuming a conical tip. In this case, the capacitance gradient in Eq. (5) is known to vary with a single logarithmic function  $\partial C/\partial z = b \times \log(D/z)$ , where the constants  $b$  and  $D$  depend on the angle and length of the cone<sup>15</sup>. Although this experiment was done near resonance frequency, the good matching indicates



that the conical tip model is a good approximation in the noncontact regime.<sup>15,16</sup> They are determined to be 1.9 nN/V<sup>2</sup> and 1000 nm, respectively, from the predictive amplitude curve (dashed line). This result suggests that  $\partial C/\partial z$  in the numerator  $F_C(z, V_{ac})$  in equation (3) contributes more to the  $X_{2\omega}$  amplitude than the denominator due to the change of  $F'_C(z, V_{ac})$  with  $z$  when the tip approaches the surface. The observed feedback stability is originated from the logarithmic long-range electrostatic interaction during the image acquisition of magnetic domains in the electrostatic force driven MFM. The contrast mechanism during the image acquisition of magnetic domain in the electrostatic force modulation results from the long-range electrostatic servo interaction that depends on the tip-sample distance  $z$  logarithmically.

In the case of the bimorph driven system, the equation of motion (1) has  $F_C = \frac{1}{2} \frac{\partial C}{\partial z} V_{dc}^2$ . The bimorph driven modulation can be described as follows:

$$u = u_0 + ae^{i\omega t} \quad (7)$$

where  $u_0$  is the midpoint of the un-deflected cantilever position,  $a$  is the driving amplitude and  $\omega$  is the angular frequency. For bimorph driven modulation, the in-phase component is predicted as follows:

$$X_\omega = \frac{a\omega_0^2}{Q} \frac{a\omega_0^2(\omega_0'^2 - \omega^2)}{(\omega_0'^2 - \omega^2)^2 + \left(\frac{\omega\omega_0}{Q}\right)^2} \quad (8)$$

$$\text{where } \omega_0'^2 = \omega_0^2 \left( 1 - \frac{1}{k} (F'_m + F'_C(z, V_{dc})) \right), \quad \text{and}$$

$$F'_C(z, V_{dc}) = \frac{1}{2} \frac{\partial^2 C}{\partial z^2} V_{dc}^2 \quad (9)$$

This result suggests that the electrostatic force gradient  $F'_C(z, V_{dc}) \propto \frac{1}{z}$  is the origin of the servo interaction in bimorph driven modulation<sup>17</sup>. The dashed line in **Figure 5(a)** also confirms that the  $1/z$  function represents nicely over the noncontact region in the in-phase  $X_\omega$  - distance curve of the bimorph driven system. This result shows that, in the bimorph driven system, the in-phase vibration amplitude  $X_\omega$  is controlled by the change of  $F'_C(z, V_{dc})$  due to the absence of the factor  $\partial C/\partial z$  in the numerator in equation (8).

Based on the understanding of the interactions of the tip and the sample surface of **Fig. 5(a)** and **5(b)**, the separation mechanism is described through the comparison between the bimorph driven system and electrostatic force modulation system in **Fig. 6(a)** and **6(b)**. In **Fig. 6(a)**, topographic features (shaded profile) and the magnetic features (solid profile line extracted from the dotted line in **Fig. 3(a)**) appear together across the vertical dashed line due to the involvement of the short-range interaction during data acquisition. This is because the tip is likely to crash with tall topographic features during the oscillatory motion of the cantilever, as illustrated on the right side of **Fig. 6(a)**. Such a coexistence of topographic and magnetic structures on an MFM image was found to depend on the distance between tip and surface and oscillatory amplitude<sup>6</sup>. In the bimorph driven MFM, only an electric force gradient  $F'_C(z, V_{dc})$  plays this role. In the electrostatic force modulation, the bigger amplitude in  $X_{2\omega}$  at a closer distance in the noncontact region indicates that the in-phase amplitude of the  $2\omega$  component is controlled more by  $F_C(z, V_{ac})$  than by  $F'_C(z, V_{ac})$ . The change of magnetic force gradient ( $\Delta F'_m$ ) is compensated by the factor  $F_C(z, V_{ac})$  to maintain the in-phase amplitude constant under feedback through the movement of the piezo tube. In the MFM using bimorph driven modulation, the change of magnetic force



gradient ( $\Delta F_m'$ ) is simply compensated by servo force gradient<sup>2,18,19</sup>. The shorter range of the force gradient indicates that the collision can cause the excited tip to easily overcome the crossover barrier. In the electrostatic force modulation system, the long-range nature of the interaction keeps the tip from being crashed into the topographic features, as shown in **Fig. 6(b)**. Due to such long-range of interactions, the MFM image has only magnetic structures without having any topographic features as found in **Fig. 3(b)**. This is because the oscillatory amplitude is smaller than the tip-sample distance as depicted in **Fig. 6(b)**.

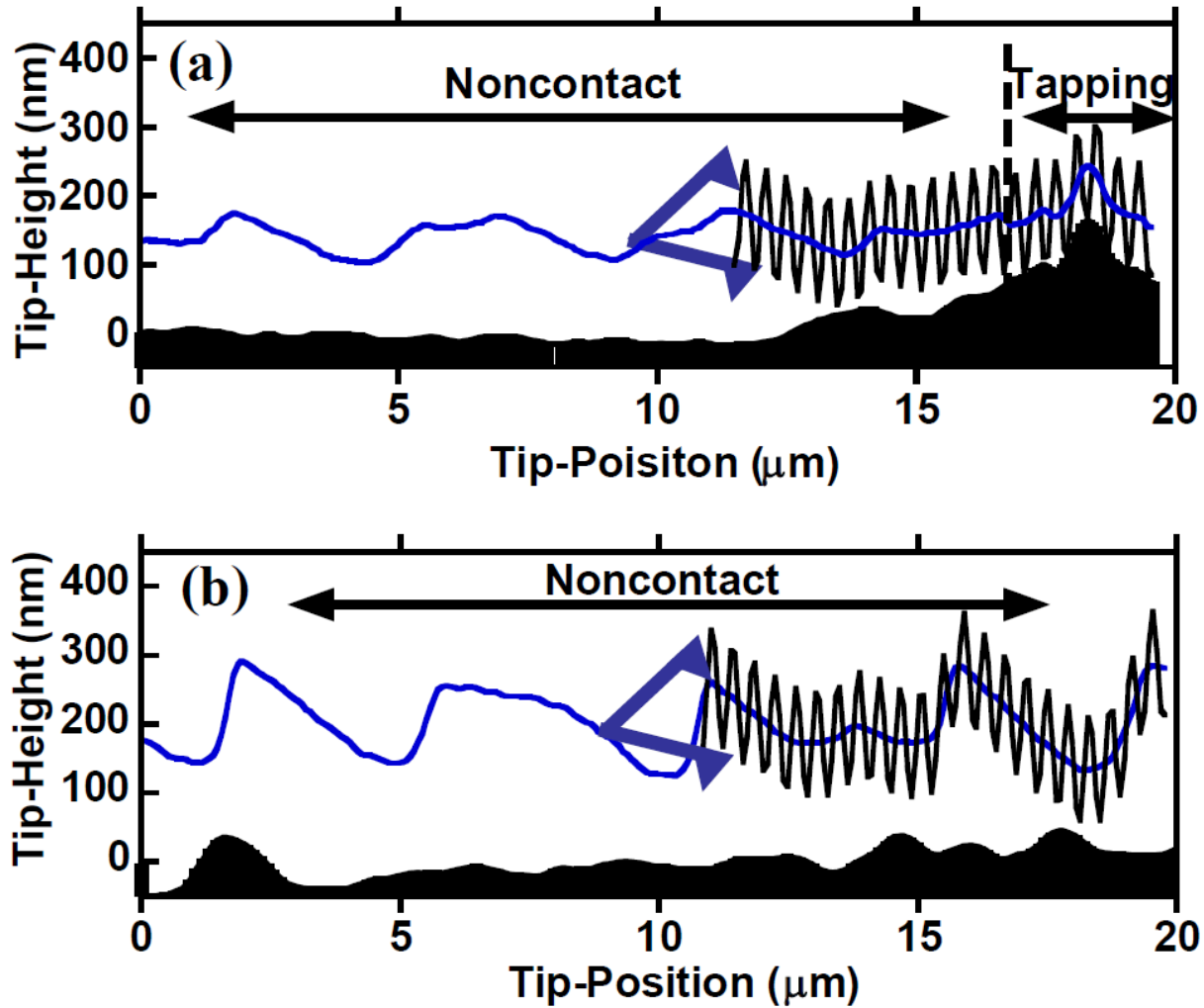


**Figure 6.** A comparison between the bimorph driven system (a) and electrostatic force modulation system (b) during the magnetic force imaging acquisition. The shaded profiles represent the topographic features, whereas the solid lines represent the sectional profiles in the magnetic force images. The oscillatory lines depict the motion of the cantilever with magnetic probes.

### Conclusion

We have developed MFM using an electrostatic force modulation that shows excellent separation of the magnetic signal from the topographic signal. We report the successful application of this system for imaging the magnetic structure and topography of CoCr thin film surfaces through separation of the magnetic and topographic structures, with enhanced stability. The system has been tested on the magnetic domain structures of CoCr magnetic film, with a periodicity of 4.5 to 5  $\mu\text{m}$ . The system has good stability due to the long-range electrostatic capacitance force and also the well-defined single resonance peak in the frequency response. Compared to the bimorph driven system, the observed magnetic images do not show any topographic features, clearly indicating the separation of topographic and magnetic signals in the noncontact

region. We attribute this separation to the opposite feedback polarity in the noncontact region to the one in tapping mode for topographic imaging, thus preventing the magnetic signal from mixing with the topographic signal under feedback condition for the constant amplitude. The origin of the feedback polarity difference is discussed with the electrostatic capacitive coupling and is compared with the bimorph driven system. This enhanced stability may come from differences between the two systems in terms of the servo forces and modulation method. We attribute the higher stability of MFM using electrostatic force modulation (instead of bimorph driven modulation) to the long-range electrostatic interaction between the tip and the sample surface. This system will be a promising tool for studying magnetic and topographic structures on the magnetic sample surfaces.

## References

- 1) Y. Martin, H.K. Wickramasinghe, *Appl. Phys. Lett.* **50**, 1455 (1987).
- 2) H.J. Güntherodt, R. Wiesendanger (eds.): *Scanning Tunneling Microscopy I-II*. (Springer: Verlag, Berlin, 1992).
- 3) S. Porthun, L. Abelmann, C. Lodder, *J. Magn. Magn. Mater.* **182**, 238 (1998).
- 4) X. Zhu, P. Grütter, V. Metlushko, B. Ilic, *Phys. Rev. B* **66**, 024423 (2002).
- 5) B.I. Kim, J.W. Hong, J.I. Kye, Z.G. Khim, *J. Korean. Phys. Soc.* **31**, s79 (1997). doi: 10.3938/jkps.31.79
- 6) B.I. Kim, *Rev. Sci. Instrum.* **80**, 023702 (2009).
- 7) H.J. Mamin, D. Rugar, J.E. Stern, B.D. Terris, S.E. Lambert, *Appl. Phys. Lett.* **53**, 1563 (1988).
- 8) R. Garcia, A. San Paulo, *Ultramicroscopy* **82**, 79 (2000a).
- 9) Q. Zhong, D. Inniss, K. Kjoller, V.B. Elings, *Surf. Sci. Lett.* **290**, L688 (1993).
- 10) R. Garcia, A. San Paulo, *Phys. Rev. B* **61**, R13381 (2000b).
- 11) B.N.J. Persson, *Sliding Friction: Physical Principles and Applications*, 2nd ed. (Springer, Heidelberg, 2000), pp. 54-77.
- 12) B. Anczykowski, D. Kruger, H. Fuchs, *Phys. Rev. B* **53**, 15485 (1996).
- 13) A. Kuhle, A.H. Sorensen, J.B. Zandbergen, J. Bohr, *Appl. Phys. A: Solids Surf.* **66**, S329 (1998).
- 14) J.W. Hong, Z.G. Khim, A.S. Hou, S.I. Park, *Appl. Phys. Lett.* **69**, 2831 (1996).
- 15) H. Yokoyama, T. Inoue, J. Itoh, *Appl. Phys. Lett.* **65**, 3143 (1994).
- 16) S. Belaidi, P. Girard, and G. Leveque, *J. Appl. Phys.* **81**, 1023(1997).
- 17) A.S. Hou, PhD dissertation, Stanford University at Palo Alto, CA (1995).
- 18) Y. Martin, D. Rugar, H.K. Wickramasinghe, *Appl. Phys. Lett.* **52**, 244 (1988).
- 19) A. Wadas, P. Grütter, H.J. Güntherodt, *J. Appl. Phys.* **67**, 3462 (1990).

## Figure Captions

**Figure 1.** (a) Schematic of the bimorph driven system. (b) Schematic of the electrostatic force modulation system.

**Figure 2.** Amplitude vs. frequency response for the cantilever. (a) The bimorph driven system. (b) The electrostatic force modulation system.

**Figure 3.** MFM images showing maze-like magnetic domain structures with periodicity 3 to 5  $\mu\text{m}$  (scan area: 20  $\mu\text{m}$  x 20  $\mu\text{m}$ ) taken with bimorph driven system (a) and electrostatic force modulation system (b).

**Figure 4.** (a) Transition from magnetic domain imaging mode to topographic imaging mode during tip-scanning of CoCr film with set-amplitude 85 nm using bimorph driven modulation (scan area: 40  $\mu\text{m}$  x 40  $\mu\text{m}$ ). The bimorph driven system is more susceptible to large topographic features such as the feature indicated by an arrow, which causes the imaging mode to change from magnetic to topographic. (b) Magnetic domain image of CoCr film in the noncontact regime with set-amplitude 95 nm operating at the resonance frequency 53 kHz using the electrostatic force modulation system (scan area: 40  $\mu\text{m}$  x 40  $\mu\text{m}$ ). The system is robust against frequent tip-collisions with topographic hillocks such as the feature indicated by an arrow.

**Figure 5.** (a) Amplitude vs. distance data for the bimorph system. Note the identical feedback polarity in the noncontact and tapping regions. The dashed line fits the data with  $1/z$ . (b) Amplitude vs. distance data for the electrostatic force modulation system. Note the barrier between the noncontact and tapping regions and the opposite feedback polarity (sign of slope) in each region. The dashed line fits the data to the logarithmic function  $b \times \log(D/z)$ .

**Figure 6.** A comparison between the bimorph driven system (a) and electrostatic force modulation system (b) during the magnetic force imaging acquisition. The shaded profiles represent the topographic features, whereas the solid lines represent the sectional profiles in the magnetic force images. The oscillatory lines depict the motion of the cantilever with magnetic probes.